

# **Special Issue Research Article**

# Modulating Photochemical Properties to Enhance the Stability of Electronically Dimmable Eye Protection Devices<sup>†</sup>

Sruthy Baburaj<sup>1,‡</sup>, Jayachandran Parthiban<sup>1,‡</sup>, Sarvar Aminovich Rakhimov<sup>1</sup>, Rasheedah Johnson<sup>2</sup>, Ludmila Sukhomlinova<sup>2</sup>, Paul Luchette<sup>2</sup>, Steffen Jockusch<sup>1</sup>, Malcolm D. E. Forbes<sup>1</sup> and Jayaraman Sivaguru<sup>\*1</sup>

Received 14 September 2022, accepted 20 February 2023, DOI: 10.1111/php.13795

#### **ABSTRACT**

The study evaluates compatibility of stabilizers with dye doped liquid crystal (LC) scaffolds that are used in electronically dimmable materials. The photodegradation of the materials was investigated and suitable stabilizers were evaluated to slow the degradation process. Various types of benzotriazole-based stabilizers were evaluated for stabilizing the liquid crystals. Based on spin trapping experiments, radicals generated upon UV exposure is likely responsible for the degradation of the system. The radical generation is competitively inhibited by the addition of stabilizers.

Abbreviations: LC, liquid crystal; STB, stabilizers.

# INTRODUCTION

The development of functional soft materials is of critical importance in the modern world. The properties of soft materials make it appealing for use in stimuli responsive systems. Liquid crystals (LCs) are budding soft materials, with the commercial viability in the realm of applied science (1,2). They are used as materials for light control applications because of their molecular property to assemble as partially ordered scaffolds (3). LC mixture dispersion of dichroic dyes and LC materials provide electronically controlled tint-on-demand (4). Typically, the liquid crystals are sandwiched with other layers of conductive materials and stabilizers. Mixtures of liquid crystals and dichroic dyes provide a practical technology platform for light control applications providing tint-on-demand with low power requirements (4). Their performance makes them ideal for a broad range of commercial

Light transmission levels are determined by orientation of the dye molecules dispersed in the LC. In the transmissive configuration, the dye and LC molecules are oriented parallel, on average, to the incident light. In the tinted configuration, the dye and LC molecules are oriented perpendicular to the incident light. The application of a small electric field across the LC film switches the molecules between these orientations (Fig. 1, bottom) (5–7).

Due to excited state reactions occurring in the presence of light, the activity of LC-dye mixtures is typically affected. The dye and LC mixture can absorb light and go to an excited state and can experience various excited state processes. The excited state can undergo photophysical events (emission, intersystem crossing etc.) as well as electron transfer processes that is dependent on the oxidation and reduction potential of the donor and acceptor respectively (8). Due to light absorption (by the LC or the Dye), the excited species become a strong oxidant as well as a strong reductant. The feasibility of electron transfer for such excited state is governed by the Rehm-Weller equation (Fig. 2, bottom) (9,10). Thus, a combination of excited state events can potentially initiate degradation process that undermines the integrity of the materials upon light exposure. This light-induced degradation in LC material that is used for electronically dimmable eye protection devices give rises to migration, discoloration, and performance degradation. To overcome these limitations, one has to design systems to slow the degradation rate(s) upon light exposure and increase the durability of the materials. In this report, we disclose the use of stabilizers (11) as additives that slows the degradation process and improves the durability of the electronically dimmable materials (5-7).

Dyes, LC's, and stabilizers were provided by Alphamicron Inc. Spectrophotometric solvents (purchased from Sigma-Aldrich). were used whenever necessary unless or otherwise mentioned. UV quality fluorimeter cells (with range until 190 nm) were purchased from Starna Cells, Inc. Absorbance measurements were performed using an Agilent 8452 UV–Vis spectrophotometer. The UV–Vis spectrometer was

<sup>&</sup>lt;sup>1</sup>Department of Chemistry, Center for Photochemical Sciences, Bowling Green State University, Bowling Green, OH

<sup>&</sup>lt;sup>2</sup>Material Development, Alphamicron Inc., Kent, OH

applications, ranging from eyewear to automotive and architectural markets (4).

**MATERIALS AND METHODS** 

<sup>\*</sup>Corresponding author email: sivagj@bgsu.edu (Jayaraman Sivaguru)

<sup>&</sup>lt;sup>†</sup>This article is part of a Special Issue celebrating the 50<sup>th</sup> Anniversary of the American Society for Photobiology.

<sup>&</sup>lt;sup>‡</sup>These authors contributed equally and are considered co-first authors. The co-first authors are listed based on the alphabetical order of their last names.

<sup>© 2023</sup> The Authors. *Photochemistry and Photobiology* published by Wiley Periodicals LLC on behalf of American Society for Photobiology.

This is an open access article under the terms of the Creative Commons Attribution License, which permits use, distribution and reproduction in any medium, provided the original work is properly cited.

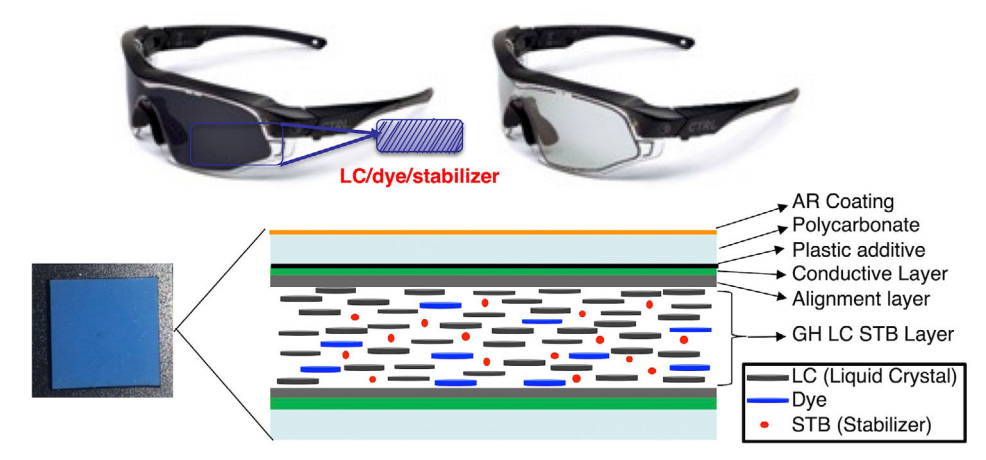
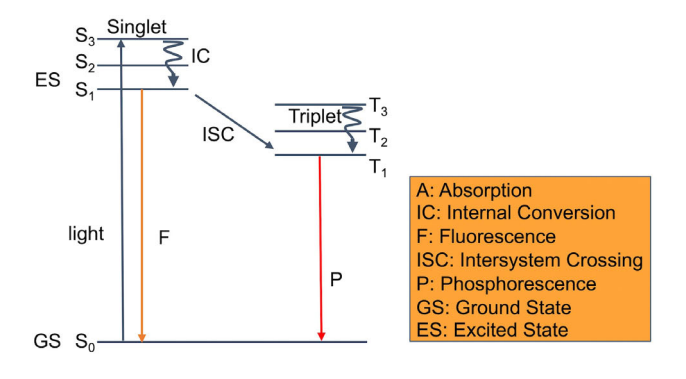
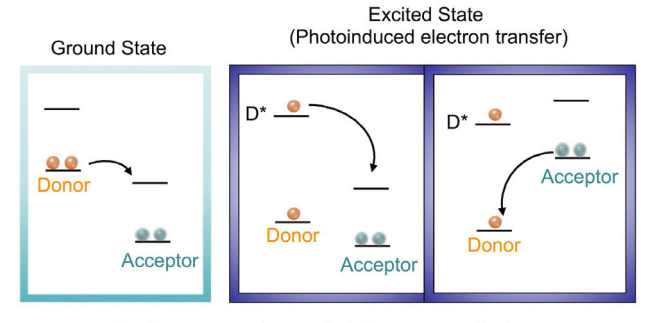


Figure 1. Visors in the ON (left) and OFF (right) states (Top). Schematic representation of a film used in visors (Bottom).





The donor can be the excited LC or the excited dye

 $\Delta G = [E_{ox} - E_{red}] - E^* - \epsilon$ 

 $\Delta G^{\circ}_{ET}$  = Free energy of electron transfer (kcal/mol);  $E_{ox}$  or  $E^{\circ}_{(D^{+}/D)}$  = Oxidation potential of electron donor (V vs Ag/Ag<sup>+</sup>);  $E_{red}$  or  $E^{\circ}_{(A/A^{-})}$  = Reduction potential of electron acceptor (V vs Ag/Ag<sup>+</sup>);  $E_{00}$  = Excitation energy (V);  $\varepsilon$  = Coulomb term

**Figure 2.** State energy diagram showing possible transitions after excitation with light (top). Representation of electron transfer in ground state (bottom left) or from the excited state of the donor (excited LC or excited the dye) to the acceptor (bottom center) or from the donor to the excited acceptor (bottom right).

modified to hold the glass-cells featuring the LC-dye and LC-dye-stabilizer materials. The holder and modification are detailed in the Supporting Information.

Cyclic voltammetry measurements were performed using PINE instruments with Epsilon software. A cell consisting of three electrodes *i.e.* Platinum wire counter electrode, glassy carbon working electrode and Ag/AgNO<sub>3</sub> (0.01 M AgNO<sub>3</sub>, 0.1 M n-Bu<sub>4</sub>N<sup>+</sup> PF<sub>6</sub><sup>-</sup> in CH<sub>3</sub>CN) as reference electrode was employed for measurements. The potential range

(solvent window) for CV measurements was determined by the solvent of choice and was kept between  $-1.8~\rm V$  to  $+1.8~\rm V$ . The conditions for honeycomb and E-Chem cells: Cyclic Voltammogram of **LC** and **Dye1** in DCM/THF/MeCN as solvent and  $n\text{-Bu}_4\text{N}^+\text{PF}_6^-$  as supporting electrolyte vs Ag/AgNO $_3$  (0.01 M AgNO $_3$  in 0.1 M  $n\text{-Bu}_4\text{N}^+\text{PF}_6^-$  in DCM/MeCN) as a reference electrode. A platinum honeycomb electrode was utilized in which the honeycomb electrode chip contains an onboard working and counter electrode. The scan rate is 100 mV s $^{-1}$ .

The EPR spectra were acquired using a JEOL, USA, Inc. JES-X310 spectrometer with the following settings: Center Field 336 mT, Sweep Width 10 mT, 100 kHz field modulation amplitude 0.1 mT, sweep time 1.0 min, time constant 0.1 s. Samples were irradiated using Continuum Surelite Nd:YAG laser of 355 nm (pulse width 10 ns, energy ~20 mJ) during EPR experiment.

Photoirradiation with medium pressure mercury lamp (chamber was customized for glass-cell irradiation) was performed with constant water flow to cool the lamp and the merry-go-round was constructed to hold the glass-cells to have uniform irradiation of the glass-cells. The glass-cells were fixed to the merry-go-round using clips. Details of the setup are provided in the Supporting Information.

### **RESULTS AND DISCUSSION**

Photodegradation is defined as chemical changes to a molecule or material caused by the absorption of photons (12). The photons can span through different wavelengths of the electromagnetic spectrum (e.g. Visible, UVA, UVB). Photodegradation in general can be broadly categorized into two types (1) direct degradation and (2) photocatalytic degradation (12). The mechanism of degradation that is initiated upon light absorption requires understanding of various excited state processes. In our study, we have investigated the photodegradation of the Liquid crystal LC and dye Dye1 with various stabilizers STB1-6 using a medium pressure mercury lamp as an irradiation source. Due to the proprietary nature of the system, the chemical structures of the materials are not disclosed in this report. The generic structure of the stabilizers STB1-6 is provided in Fig. 3A. Spectroscopic studies were carried out to evaluate the photochemical stability of dye doped liquid crystalline materials. UV-Vis spectroscopic measurements of liquid crystals (without the dye) showed that they do not absorb in the visible region. On the other hand, dve doped liquid crystals are absorbed in the visible region. Cyclic voltammetry measurements were performed on both the liquid crystal and the dye (Dye1) which showed that the LC has an oxidation potential  $(E_{ox})$  at 0.65 V and no reduction potential within the measured range, while Dye1 had an

# A) N-R

STB: R = ArOH STB1: R =  $C_{35}H_{46}O_2N_3$ STB2: R =  $C_{16}H_{25}O$ STB3: R =  $C_7H_7O$ STB4: R =  $C_{16}H_{25}O$ STB5: R =  $C_{14}H_{21}O$ STB6: R =  $C_{26}H_{21}O$ 

# B) Before Irradiation After 44h Irradiation

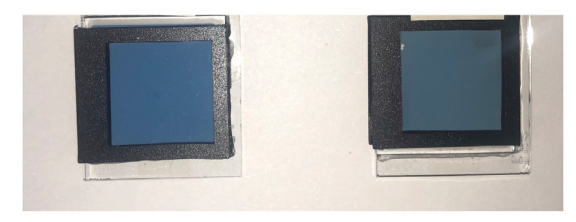


**Figure 3.** (A) Generic structures of **STB1-6**. (B) Before irradiation sample LC cell without stabilizer (left) and after 44 h irradiation sample was with medium pressure mercury (mp Hg) lamp (right).

oxidation peak  $(E_{ox})$  at 0.64 V and a reduction peak at  $(E_{red})$  at -1.04 V. Having ascertained the redox potentials, we fabricated the **LC-Dye1** mixture with stabilizers **STB1-6** (not displayed) and without stabilizers (Fig. 3B) in between glass plates. The

fabricated glass-cells were irradiated with medium pressure mercury lamp for various time intervals. During the course of the irradiation, the degradation process was monitored by UV–Visible spectroscopy (Fig. 4).

As shown in Fig. 3B, exposure of the fabricated glass-cells (LC-Dye1 materials without stabilizers that are sandwiched between glass cells) to UV light resulted in a change in the color of the glass-cell indicating degradation. This was quantified by monitoring the absorptivity of the materials before and during light exposure for various time intervals. Irradiation of LC-Dye1 system for 44 h showed a decrease in absorption at ~620 nm and an increase in absorption at ~450 nm indicating photoin-duced degradation of the material. The degradation profile was averaged by irradiating two distinct samples. The kinetics of degradation was evaluated by plotting the absorption maxima (average absorption maxima of the two samples) at ~620 nm over the irradiation time (Fig. 4D). The linear fit of the plot provided us with the rate of degradation.

To enhance the stability of the materials, we chose various stabilizers/UV-blocks to slow the rate of degradation (11). The stabilizers (STBs) were designed to undergo efficient photophysical and/or non-destructive photochemical reactions without interfering with the optical properties of the **LC-Dye1**. To assess the influence of different STBs on the LC-dye materials, we conducted a series of degradation studies with glass-cells loaded with **LC-Dye1** mixture along with different stabilizers (STBs). Six different STBs (Fig. 3A) were evaluated by employing various loading levels within the **LC-dye1** materials and their degradation profiles were evaluated by exposure to light from medium pressure mercury lamp for various time intervals (Fig. 4). The change in the absorption at 620 nm of the electronically dimmable material on the glass-cell was evaluated at various time intervals (Fig. 4). To illustrate the

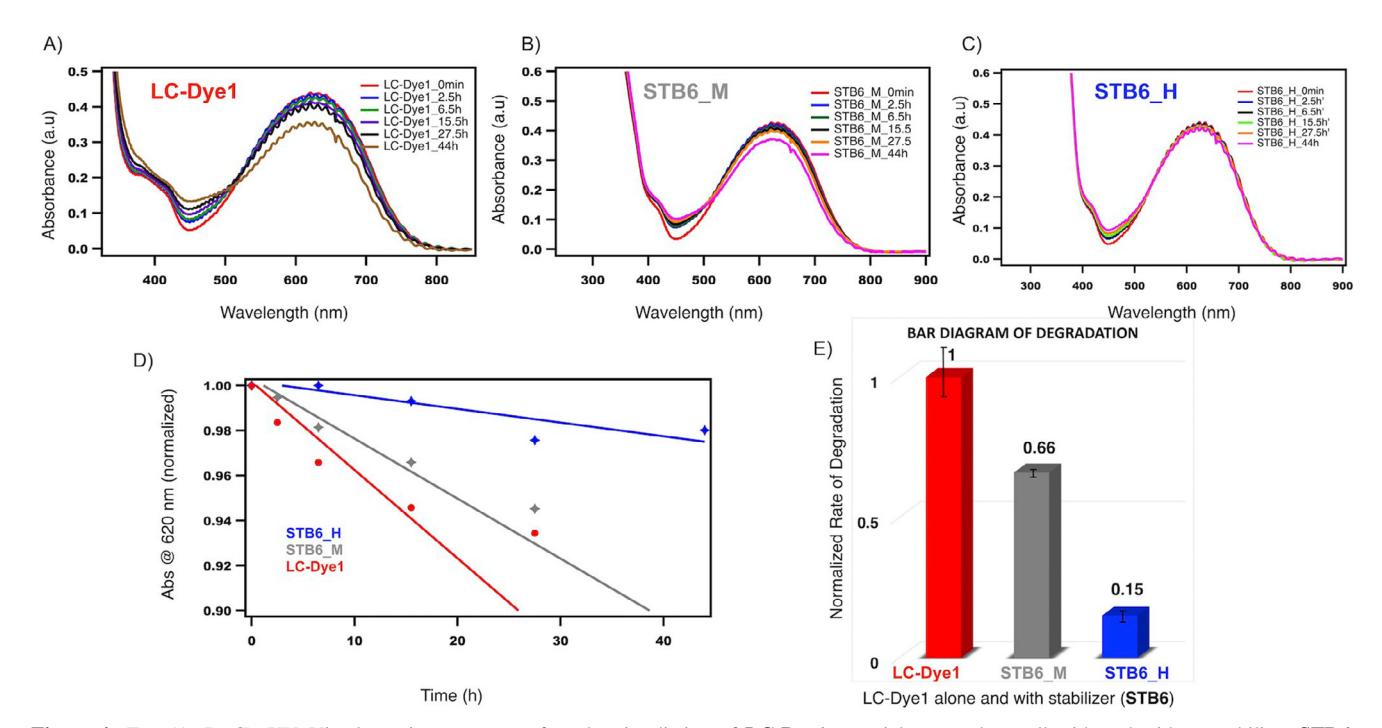


Figure 4. Top (A, B, C): UV–Vis absorption spectrum after photoirradiation of LC-Dye1 materials on a glass cell with and without stabilizer STB6. Degradation efficiency was compared with two distinct loading levels of the STB6. STB6\_M (medium loading of the stabilizer in the material), and STB6\_H (high loading of the stabilizer in the material) were employed. Ascertaining the kinetics of degradation (D) and the relative stability of the LC/dye material in the presence and absence of the stabilizer illustrated in the bar graph (E) along with error bars corresponding to the same. The experimental degradation rates are listed in Table S1.

#### 4 Sruthy Baburaj et al.

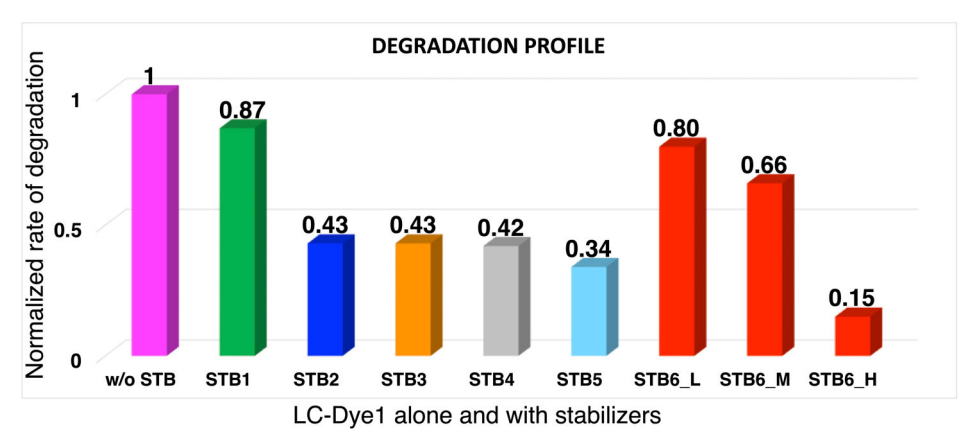
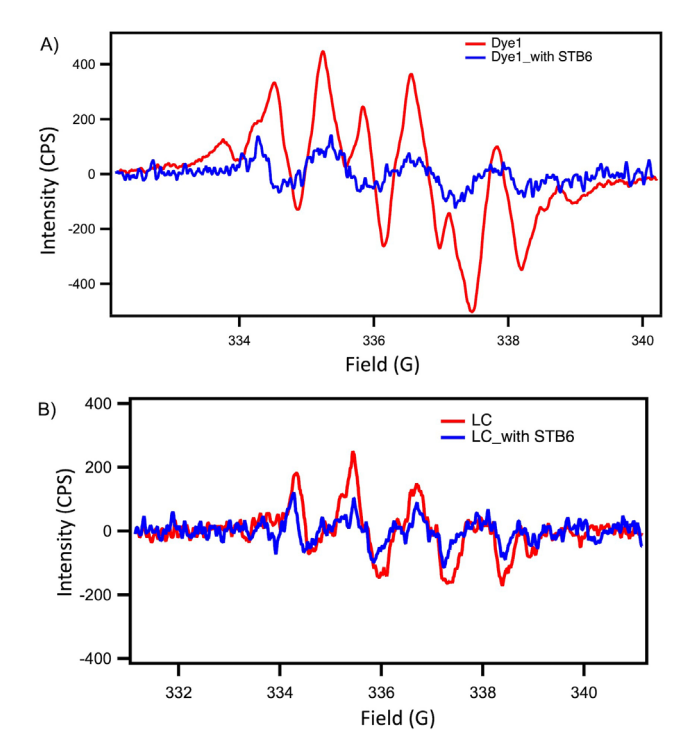


Figure 5. Degradation rate with different stabilizers STB1-6 in LC-Dye1 relative to the degradation of LC-Dye1 without STB (considered as 1). In the case of STB6 three distinct loading levels were employed STB6\_L (low loading of the stabilizer in the material), STB6\_M (medium loading of the stabilizer in the material) and STB6\_H (high loading of the stabilizer in the material). The experimental degradation rates are listed in Table S1.

influence of the various evaluated stabilizers, we will highlight the stability of the materials with stabilizer STB6 that were employed at different loading levels. The concentration of stabilizer STB6 employed in LC-Dye1 is (1) 0.5 w/w% - labeled as low loading (STB6\_L) (2) 1 w/w% – labeled as medium loading (STB6\_M), and (3) 2 w/w%- labeled as high loading (STB6\_H). The slope of the degradation profile provides relative stability of the LC-Dye1 material in the presence and absence of the stabilizer which is illustrated in the bar graph with an error bar (Fig. 4E). Keeping the degradation profile in the absence of the stabilizer as a reference, the degradation can be compared for gauging the efficiency of stabilization (shallower the slope, slower the degradation; Fig. 4D). In the case of STB6\_M the materials were ~1.5 more stable than in the absence of the stabilizer (0.66 compared to 1; Fig. 4E) which are reproducible. When a higher loading level of the stabilizer was employed viz., STB6 H the materials were ~6.6 more stable than in the absence of the stabilizer (0.15 compared to 1; Fig. 4E). All of the above photodegradation experiments (Fig. 4A-C) were carried out with duplicates and averaged for plotting.

As the loading level (based on weight %) had a significant impact on the stabilization of electronically dimmable materials we evaluated the degradation profile (Fig. 5) of various stabilizers STB1-6 (1 w/w%) loaded in LC-Dye1. Inspection of Fig. 5 shows that this class of stabilizers is effective in slowing the degradation without advert effect in the desired properties of electronically dimmable materials. Stabilizer STB1 was the least effective compared to other stabilizers with STB5 being the most effective for a given loading level (based on weight %). Of point to note is that the stabilizer selected needs to be compatible with the LC/dye system *i.e.* there should not be phase separation of the evaluated stabilizer. Clearly, the new set of stabilizers improves the stability of the LC/dye in the glass-cells that are employed for electronically dimmable eyewear.

Electron Paramagnetic Resonance (EPR) spectroscopy was performed to investigate the possible presence of free radicals and their activity toward **LC** and **Dye1**. These experiments were carried out using 5,5-dimethyl-1-pyrroline N-oxide (DMPO) as a spin trapping agent (see Supporting Information for details). A strong EPR signal was observed (Fig. 6) upon UV irradiation at 355 nm for both the **LC** material and **Dye1** (studied independently). Irradiation of **Dye1** in the presence of DMPO showed an



**Figure 6.** (A) EPR signal of **Dye1** with and without **STB6** in benzene (B) EPR signal of **LC** with and without **STB6** in benzene, DMPO was used as the radical trap reagent with 355 nm irradiation.

EPR signal indicating (Fig. 6A) the generation of a trapped radical species. Addition of stabilizer STB6 to Dye1 led to a decrease in the generation of the radicals as indicated by the decrease in intensity of the EPR signal. Irradiation of LC in the presence of DMPO again showed evidence of radical generation (Fig. 6B). This indicates that the degradation of Dye1 within the liquid crystals upon exposure to UV light likely involves the generation of free radicals. In the presence of stabilizer STB6, the radical generation is inhibited due to competitive UV absorption of the stabilizer along with a non-destructive photoprocess that dissipates the excess energy from the stabilizer.

### **CONCLUSIONS**

Our study has showcased that photophysical and photochemical studies can be utilized to enhance the properties of materials. In the present case, we have utilized stabilizers to enhance the durability of electronically dimmable systems that uses liquid crystalline materials. The stabilizers with specific photochemical features were chosen to enhance the stability and not adversely affect the performance of the systems. We observed that the loading level of a given stabilizer has a significant impact improving the stability. Further investigations are underway to understand the mechanistic, photophysical and photochemical properties of these systems to tailor them for various applications.

Acknowledgement—The research was funded by Air Force Research Laboratory, Airman Systems Directorate contract FA8649-20-C-0011 and its associated Ohio Federal Research Network 11227-004.

## **AUTHOR CONTRIBUTIONS**

The manuscript was written through the contributions of all authors. All authors have given approval for the final version of the manuscript.

#### **ENDNOTE**

§ Due to the proprietary nature of the system, the chemical structures of the materials are not disclosed in this report which was indicated to the editor prior to submission of the manuscript.

# SUPPORTING INFORMATION

Additional supporting information may be found online in the Supporting Information section at the end of the article:

**Figure S1.** Modified holder for the chip to perform UV-Vis studies.

Figure S2. Preparation of the chip irradiation set up.

Figure S3. CV of LC with platinum honeycomb against Ag/AgNO<sub>3</sub> in MeCN.

**Figure S4.** CV of **Dye1** with platinum honeycomb against Ag/AgNO<sub>3</sub> in DCM.

Figure S5. Photodegradation of LC-Dye1 with stabilizer STB1.

Figure S6. Photodegradation of LC-Dye1 with stabilizer STB2.

Figure S7. Photodegradation of LC-Dye1 with stabilizer STB3.

Figure S8. Photodegradation of LC-Dye1 with stabilizer STB4.

Figure S9. Photodegradation of LC-Dye1 with stabilizer STB5.

Figure S10. Photodegradation of LC-Dye1 with stabilizer STB6 L.

Figure S11. Photodegradation of LC-Dye1 with stabilizer STB6 M.

**Figure S12.** Photodegradation of **LC-Dye1** with stabilizer **STB6\_H**.

**Figure S13.** Time *vs* Absorbance at 620 nm for stabilizers **STB1-6**.

**Figure S14.** EPR signal of LC with and without **STB6**. DMPO was used as the radical trapping

agent with 355 nm irradiation in benzene solution.

**Figure S15.** EPR signal of **Dye1** with and without **STB6**. DMPO was used as the radical trapping agent with 355 nm irradiation in benzene.

Table S1. Rate of degradation of LC-Dye1 with and without STB1-6.

## **REFERENCES**

- Hsiang, E.-L., Z. Yang, Q. Yang, Y.-F. Lan and S.-T. Wu (2021) Prospects and challenges of mini-LED, OLED, and micro-LED displays. J. Soc. Inf. Disp. 29(6), 446–465.
- Arines, J. (2009) Impact of liquid crystals in active and adaptive optics. *Materials* 2(2), 549–561.
- Bisoyi, H. K. and Q. Li (2022) Liquid crystals: Versatile selforganized smart soft materials. *Chem. Rev.* 122(5), 4887–4926.
- Taheri, B., P. Palffy-Muhoray, T. Kosa and D. L. Post (2000) Technology for electronically varying helmet visor tint. In *Helmet- and Head-Mounted Displays V*, Vol. 4021, pp. 114–119. SPIE, Orlando, FL.
- Caillaud, B., L. Dupont, P. Gautier, J.-L. de Bougrenet de la Tocnaye, P. Rudquist, D. Engström, P. Jägemalm and S. T. Lagerwall (2008) A new application of ferroelectric liquid crystals: Fast Electrooptic helmet visors for pulsed welding applications. *Ferroelectrics* 364(1), 66–71.
- Bhatta, S., Soto, P. C., Kosa, T. and Taheri, B. (2018) Electronically switchable optical device with a multi-functional optical control apparatus and methods for operating the same. US10095052B2.
- Palffy-Muhoray, P., Kosa, T. and Taheri, B. (2001) Variable light attentuating dichroic dye guest-host device. US6239778B1.
- Turro, N. J., V. Ramamurthy and J. C. Scaiano (2010) Energy and electron transfer. In *Modern Molecular Photochemistry of Organic Molecules*, pp. 383–481. University Science Books, Sausalito, CA.
- Rehm, D. and A. Weller (1970) Kinetics of fluorescence quenching by electron and H-atom transfer. Isr. J. Chem. 8(2), 259–271.
- Farid, S., J. P. Dinnocenzo, P. B. Merkel, R. H. Young, D. Shukla and G. Guirado (2011) Reexamination of the Rehm–Weller data set reveals electron transfer quenching that follows a Sandros–Boltzmann dependence on free energy. J. Am. Chem. Soc. 133(30), 11580–11587.
- Brostow, W., X. Lu, O. Gencel and A. T. Osmanson (2020) Effects of UV stabilizers on polypropylene outdoors. *Materials* 13(7), 1626.
- Pingmuang, K., J. Chen, W. Kangwansupamonkon, G. G. Wallace and S. Phanichphant (2017) Composite photocatalysts containing BiVO4 for degradation of cationic dyes. Sci Rep. 7, 2045–2322.